

Kinetic measurements and quantum chemical calculations on low spin Ni(II)/(III) macrocyclic complexes in aqueous and sulphato medium

ANURADHA SANKARAN^{a,b}, E J PADMA MALAR^{c,*} and VENKATAPURAM RAMANUJAM VIJAYARAGHAVAN^{a,*}

^aDepartment of Physical Chemistry, University of Madras, Guindy Campus, Chennai 600 025, India

^bDepartment of Chemistry, PSNA College of Engineering and Technology, Kothandaraman Nagar, Dindigul 624 622, India

^cNational Centre for Ultrafast Processes, University of Madras, Taramani Campus, Chennai 600 113, India
e-mail: smradha73@gmail.com; ejpmalar@yahoo.com; vijju47@yahoo.co.in

MS received 13 February 2015; revised 6 April 2015; accepted 10 April 2015

Abstract. Cu(II) ion catalyzed kinetics of oxidation of H₂O₂ by [Ni^{III}L₂] (L₂ = 1,8-bis(2-hydroxyethyl)-1,3,6,8,10,13-hexaazacyclotetradecane) was studied in aqueous acidic medium in the presence of sulphate ion. The rate of oxidation of H₂O₂ by [Ni^{III}L₂] is faster than that by [Ni^{III}L₁] (L₁ = 1,4,8,11-tetraazacyclotetradecane) in sulphate medium. DFT calculations at BP86/def2-TZVP level lead to different modes of bonding between [NiL]^{II/III} and water ligands (L = L₁ and L₂). In aqueous medium, two water molecules interact with [NiL]^{II} through weak hydrogen bonds with L and are tilted by ~23° from the vertical axis forming the dihydrate [NiL]²⁺.2H₂O. However, there is coordinate bond formation between [NiL₁]^{III} and two water molecules in aqueous medium and an aqua and a sulphato ligand in sulphate medium leading to the octahedral complexes [NiL₁(H₂O)₂]³⁺ and [NiL₁(SO₄)(H₂O)]⁺. In the analogous [NiL₂]^{III}, the water molecules are bound by hydrogen bonds resulting in [NiL₂]³⁺.2H₂O and [NiL₂(SO₄)]⁺.H₂O. As the sulphato complex [NiL₂(SO₄)]⁺.H₂O is less stable than [NiL₁(SO₄)(H₂O)]⁺ in view of the weak H-bonding interactions in the former it can react faster. Thus the difference in the mode of bonding between Ni(III) and the water ligand can explain the rate of oxidation of H₂O₂ by [Ni^{III}L] complexes.

Keywords. Ni(III) macrocyclic complexes; kinetics; density functional theory; BP86; def2-TZVP; hydrogen bonding

1. Introduction

Ni(III) complexes are useful model systems to explore the properties of nickel containing enzymes.¹ The complexes [Ni^{II}L₁] and [Ni^{III}L₁], where L₁ = 1,4,8,11-tetraazacyclotetradecane (cyclam), are thermodynamically very stable species.^{2–4} High spin Ni(II) macrocyclic complexes with two axially coordinated aqua ligands have been characterized in earlier studies.^{5–12} In these high spin triplet state complexes, the axial ligands are elongated and act as hydrogen bond donors or acceptors through inter / intramolecular fashion. Fabbrizzi *et al.*^{13–15} reported that the nickel cyclam complex [Ni^{II}L₁] existed in aqueous solution as an equilibrium mixture of high-spin diaquo octahedral species [NiL₁(H₂O)₂]²⁺ and low-spin diamagnetic square planar species. Addition of NaClO₄ led to the isolation of the low-spin square-planar species [Ni^{II}L₁](ClO₄)₂.¹⁶ The X-ray crystallography and single crystal vis-absorption spectrum of *trans*-[Ni

(OH₂)₂(cyclam)]Cl₂.4H₂O show that two water molecules axially coordinate to the central Ni(II) ion in the high-spin state.⁵ The average Ni-N and Ni-O bond lengths in the above octahedral geometry are 2.069 and 2.176 Å respectively.⁵ Hydrogen bond net work from the hydrated water molecules and the uncoordinated chlorine atoms in the above complex plays a role in stabilizing the coordination of the two axial aqua ligands to the central Ni(II) ion.⁵ Ito *et al.* reported that in aqueous solutions or solutions of organic solvents containing water, hydrations take place around N-H groups in the macrocyclic ligand.¹⁷ In the complex [Ni(meso-Me₆[14]aneN₄)]Cl₂.2H₂O coordination of water as well as chloride ion is prevented in the aqueous medium due to specific hydrogen-bond effect which results in low-spin four coordinate complex.¹⁷ Axially coordinated Ni(III) complexes exist in the low spin state with one unpaired electron as evidenced by magnetic moment and EPR measurements.¹⁸

Ni(III) complexes play important role in catalytic oxidation reactions.^{19–24} Redox reactions of

*For correspondence

nickel(II/III) macrocyclic complexes still continue to be a subject of interest. Gore and Busch reported that axial coordination of simple ligands stabilizes Ni(III) complexes dramatically.¹⁸ The stability of Ni(III) aza-macrocyclic complexes in solutions is influenced by pH, nature of solvent, the type of anion apically coordinated to the Ni(III) centre and the structure of the complex. Meyerstein and coworkers have shown that simple inorganic anions coordinated axially to the Ni centre stabilize the Ni(III) oxidation state in complexes with 14-membered N4 macrocyclic ligands.^{25–29} Organic ligands such as the aromatic carboxylates form intra/intermolecular hydrogen bonding interactions with Ni cyclam complexes and function as good candidates for the construction of multi-dimensional coordination polymers.^{11,12,30–32} Zilbermann *et al.*³³ studied the stabilization of Ni(III) in 1,8-dimethyl-1,3,6,8,10,13-hexaazacyclotetradecane by axial binding of anions in neutral aqueous solutions.

We have recently reported the kinetics of catalytic oxidation of hydrogen peroxide by Ni(III) tetra-aza macrocycle in acidic aqueous solution.³⁴ The reduction of metal centre was complicated by the simultaneous ligand oxidation by hydrogen peroxide. The $[\text{Ni}^{\text{II}}\text{L}_1]$ to $[\text{Ni}^{\text{III}}\text{L}_1]$ reduction was found to be faster in presence of Cu(II) ion than the oxidation of cyclam ligand by $\bullet\text{OH}$ in aqueous acidic medium. The presence of sulphate retards oxidation of H_2O_2 due to the stabilization of $[\text{Ni}^{\text{III}}\text{L}_1]$ by forming $[\text{NiL}_1(\text{H}_2\text{O})(\text{SO}_4)]^+$. The rate constant for the reaction $[\text{NiL}_1(\text{H}_2\text{O})(\text{SO}_4)]^+ / \text{H}_2\text{O}_2$ at pH 1 was calculated as $17 \text{ dm}^3\text{mol}^{-1}\text{s}^{-1}$ in the presence of sulphate concentration of $0.002 \text{ mol dm}^{-3}$. In the present paper, we report the copper catalysed oxidation of hydrogen peroxide by Ni(III) hexa-aza macrocycle, $[\text{Ni}^{\text{III}}\text{L}_2]$ ($\text{L}_2 = 1,8\text{-bis}(2\text{-hydroxyethyl})\text{-}1,3,6,8,10,13\text{-hexaazacyclotetradecane}$) in acidic aqueous solution in the presence of excess sulphate. The rate constant for the hydrogen peroxide oxidation is higher in $[\text{Ni}^{\text{III}}\text{L}_2]$ than that in $[\text{Ni}^{\text{III}}\text{L}_1]$. This observation has initiated us to study the nature of bonding in these complexes in aqueous and sulphato medium by DFT calculations. The structure of the ligands L_1 and L_2 is shown in scheme 1.

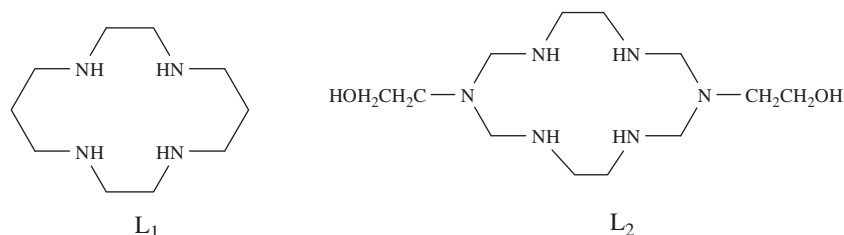
The Ni(III) species with axial coordination of the solvent or counter-ions possess elongated geometry as confirmed by hyperfine interactions.^{3,25} The tricationic Ni(III)-aza-macrocyclic complexes are considered to exist as $[\text{NiL}(\text{H}_2\text{O})_2]^{3+}$ and $[\text{NiL}(\text{H}_2\text{O})(\text{SO}_4)]^+$ in aqueous and sulphato medium respectively.²⁹ Though $[\text{Ni}(\text{cyclam})]^{3+}$ was synthesized and its crystal structure was rationalised,³⁵ the structure of the trivalent complexes $[\text{NiL}(\text{H}_2\text{O})_2]^{3+}$ and $[\text{NiL}(\text{H}_2\text{O})(\text{SO}_4)]^+$ ($\text{L} = \text{L}_1$ and L_2) were not studied so far.

In the present study, we have examined the structure and bonding of $[\text{Ni}^{\text{II}}\text{L}]$ in aqueous medium and $[\text{Ni}^{\text{III}}\text{L}]$ in aqueous and sulphato medium by Density Functional Theory (DFT) computations. Although the existence of equilibrium between high and low spin $[\text{Ni}^{\text{II}}\text{L}]$ in aqueous medium under different conditions is examined in earlier studies,^{15–17} in the presence of perchlorate it was found to exist in the low-spin form.^{16,36} The electronic spectra of $[\text{Ni}^{\text{II}}\text{L}]$ complexes in aqueous medium show absorption band with $\lambda_{\text{max}} = 444 \text{ nm}$ which corresponds to low spin square planar complex.^{37,38} Therefore, in the present study we have investigated the electronic and geometric structures of the low-spin $[\text{Ni}^{\text{II}}\text{L}]$ complexes in aqueous medium. We have studied the closed-shell singlet state with all paired electrons that results in the diamagnetic system. The $[\text{Ni}^{\text{III}}\text{L}]$ complexes possess one unpaired electron and are in the doublet state.¹⁸ The bonding between the Ni ion and water/sulphato ligand was investigated by orienting the water/sulphato ligand in the axial position initially and subjecting it to complete structural optimization. At the optimized geometries, the nature of bonding between the Nickel ion and the ligands were examined. The correlation between the bonding mode and reactivity of the $[\text{Ni}^{\text{III}}\text{L}]$ complexes in aqueous and sulphato medium is reported in the present work.

2. Experimental

2.1 Materials and reagents

$[\text{Ni}^{\text{II}}\text{L}_2](\text{ClO}_4)_2$ and the corresponding $[\text{NiL}_2(\text{Br}_2)]\text{ClO}_4 \cdot 2\text{H}_2\text{O}$ complexes were prepared as described



Scheme 1. Structure of the macrocyclic ligands.

earlier.^{34,37,39} The UV spectrum of $[\text{NiL}_2](\text{ClO}_4)_2$ in aqueous solution ($\epsilon_{444} = 54 \text{ M}^{-1} \text{ cm}^{-1}$, $\epsilon_{205} = 15,300 \text{ M}^{-1} \text{ cm}^{-1}$), Ni(III) complex in acetonitrile ($\epsilon_{381} = 7500 \text{ M}^{-1} \text{ cm}^{-1}$, $\epsilon_{291} = 10,600 \text{ M}^{-1} \text{ cm}^{-1}$) and the ESR spectrum in aqueous acidic medium in the presence of excess sulphate at 77K were used for characterising the complex. The $[\text{Ni}^{\text{III}}\text{L}_2]$ solution was prepared freshly by dissolving the sample in aqueous acidic solution containing sulphate. A stock solution of perchloric acid was prepared and was standardised by titration with potassium hydrogen phthalate. The pH was measured with a Eutech India pH meter. Sodium perchlorate (Loba Chemie, India) was purchased and used as such to maintain the ionic strength. A stock solution of copper perchlorate was prepared by neutralizing copper carbonate (0.0091 mole, 2 gram) with 70% perchloric acid (1.56 ml, 0.018 mole). The resultant solution was standardized iodometrically.

Caution: Compounds containing perchlorate anion must be regarded as potential explosives and should be handled with caution.

2.2 Computational

The molecular structures and bonding in the low-spin nickel complexes $[\text{Ni}^{\text{II}}\text{L}]$ in aqueous medium and $[\text{Ni}^{\text{III}}\text{L}]$ in aqueous and sulphato medium ($\text{L}=\text{L}_1$ and L_2) were investigated using DFT computations. The complexes are represented as **1** $\text{Ni}^{\text{II}}\text{L}_1(\text{H}_2\text{O})_2$, **2** $\text{Ni}^{\text{III}}\text{L}_1(\text{H}_2\text{O})_2$, **3** $\text{Ni}^{\text{III}}\text{L}_1(\text{SO}_4)(\text{H}_2\text{O})$, **4** $\text{Ni}^{\text{II}}\text{L}_2(\text{H}_2\text{O})_2$, **5** $\text{Ni}^{\text{III}}\text{L}_2(\text{H}_2\text{O})_2$, and **6** $\text{Ni}^{\text{III}}\text{L}_2(\text{SO}_4)(\text{H}_2\text{O})$. We performed complete structural optimization with the BP86 functional⁴⁰ using Aldrich's extended Triple zeta valence basis set def2-TZVP⁴¹ including the auxiliary def2-TZVP/J basis set. The BP86 functional yields reliable results in transition metal chemistry.^{42,43} The def2-TZVP basis set includes valence triple-zeta plus 1p polarisation (TZVP) for hydrogen and additional polarization function on the main group elements (TZVPP) and this basis is expected to yield accurate results.⁴¹ To enhance the efficiency of the calculations, the combination of the resolution of the identity (RI) and the "chain of spheres exchange" algorithms (RIJCOSX)⁴⁴⁻⁴⁸ were employed. The computations were carried out using the ORCA 3.0.0 software.⁴⁹

The role of aqueous medium was studied using the "COnductor-like Screening MOdel" (COSMO) method⁵⁰ which approximates the solvent surrounding the solute molecule by a dielectric continuum. The electrostatic interaction between the solute molecule and the solvent medium with permittivity ϵ is calculated

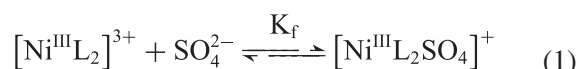
using the polarized continuum model (PCM). The non-covalent dispersion interactions acting in the complexes were computed by the third generation dispersion correction (D3) developed by Grimme *et al.* including the Becke-Johnson damping (D3BJ) method.^{51,52} Covalent bond orders obtained by Mayer population analysis⁵³ were used to examine the bonding between the nickel ion and the ligand. The complexes were also studied in the gas-phase at BP86/def2-TZVP level using the ORCA software⁴⁹ and at B3LYP/6-31+G* level⁵⁴ using the Gaussian software.⁵⁵

2.3 Kinetic studies

Kinetics of oxidation of hydrogen peroxide by $[\text{NiL}_2(\text{SO}_4)]^+$ under first and second order conditions were carried out in the presence of sulphate ion. Ionic strength was maintained at 0.5 mol dm^{-3} using sodium perchlorate. The concentration of H_2O_2 was varied from 2.5×10^{-4} to $1 \times 10^{-3} \text{ mol dm}^{-3}$ and the Ni(III) complex concentration was fixed at $5 \times 10^{-5} \text{ mol dm}^{-3}$. The concentration of $[\text{Cu}(\text{II})]$ was fixed at $1 \times 10^{-4} \text{ mol dm}^{-3}$. Sulphate concentration of $0.005 \text{ mol dm}^{-3}$ was used to stabilize the complex in aqueous medium. The pH dependence on the reaction rate was studied by varying the pH between 1 and 2.5, using perchloric acid. Absorbance changes with time were measured using a "Shimadzu" UV-Visible recording spectrophotometer (UV-1601). Decrease in absorbance of LMCT band of Ni(III) was followed at 350 nm. The observed rate constant k_{obs} was calculated from the slopes of the linear regression plots of $\ln\{1+(Y_o-Y_\infty)\Delta_o/(Y_t-Y_\infty)[A]_o\}$ (where $\Delta_o = a[B_o] - b[A_o]$; $[A_o]$ and $[B_o]$ are initial concentrations of oxidant and reductant respectively) against time for second order and $\ln(Y_t-Y_\infty)$ against time for first order conditions.⁵⁶ Y_o and Y_∞ denote the initial and final absorbance of the oxidant and Y_t is the absorbance at time t .

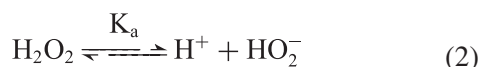
3. Results and Discussion

In order to examine the redox behaviour of $[\text{Ni}^{\text{III}}\text{L}_2]$, sulphate concentration of $0.005 \text{ mol dm}^{-3}$ was maintained in the pH range $1 < \text{pH} < 2.5$. In sulphate medium,⁵⁷ $[\text{Ni}^{\text{III}}\text{L}_2]$ exist as sulphato-complex according to the Equation (1)

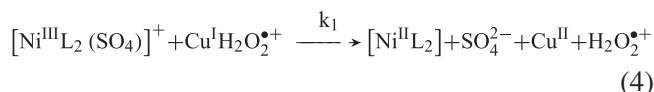
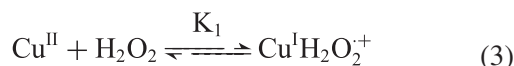


Negligible intercepts are reported in $[\text{M}(\text{bipy})_3]^{3+} / \text{H}_2\text{O}_2$ (where $\text{M} = \text{Ni}, \text{Fe}, \text{Ru}$) reaction in acidic

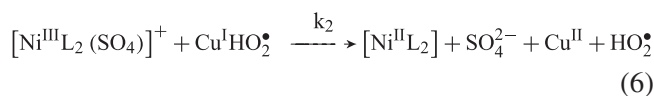
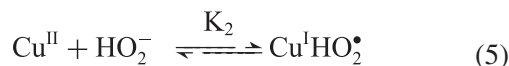
solution.⁵⁸ With $[\text{Ni}(\text{tacn})_3]^{3+}$, HO_2^- is the only redox-active species and reduction occurs only at metal centre and not at the ligand.⁵⁹ Kinetic measurements of oxidation of hydrogen peroxide by $[\text{Ni}^{\text{III}}\text{L}_2(\text{SO}_4)]$ was found to be complicated and the uncatalysed reaction may involve ligand oxidation similar to $[\text{Ni}^{\text{III}}\text{L}_1(\text{SO}_4)]$.³⁴ The peroxy anion, HO_2^- , formed by dissociation of hydrogen peroxide (eq. 2) may react with metal complex to form a stable oxidant $[\text{Ni}^{\text{III}}\text{L}_2\text{HO}_2^-]$.



The metal centred reduction reaction was substantiated in presence of Cu(II) ion. Most of the reactions involving hydrogen peroxide are carried out at higher pH ($\text{pH} > 5$) and HO_2^- is responsible for the decomposition of H_2O_2 . The oxidation of H_2O_2 by Cu(II) is more favourable in alkaline medium and the rate of decomposition of H_2O_2 by Cu(II) ion alone at low pH is considered negligible when compared with the decomposition of H_2O_2 by Ni(III) complex.³⁴ Interaction of $[\text{Cu}(\text{II})]$ with $[\text{Ni}^{\text{III}}\text{L}_2]$ complexes in aqueous acidic condition was ruled out.⁶⁰ At lower pH the hydrogen peroxide is activated by copper(II) ion and the catalytic action of Cu(II) is due to its ready reducibility to Cu(I) as reported earlier.^{61,62} In aqueous acidic medium, highly labile species $\text{Cu}^{\text{I}}\text{H}_2\text{O}_2^{\bullet+}$ is formed³⁴ (eq. 3) and it participates in electron transfer reaction with $[\text{Ni}^{\text{III}}\text{L}_2(\text{SO}_4)]$ as represented by the rate expression (4)



The peroxy anion can react with Cu(II) and the $[\text{Cu}^{\text{II}}\text{HO}_2^-]$ or $[\text{Cu}^{\text{I}}\text{HO}_2^{\bullet}]$ formed reacts with $[\text{Ni}^{\text{III}}\text{L}_2(\text{SO}_4)]$. The rate equation for the Cu(II) ion promoted peroxy anion may be given by the Equation (6).



The metal centred reduction takes place more readily when compared with ligand oxidation.³⁴ The rate

expression for the oxidation of H_2O_2 by $[\text{Ni}^{\text{III}}\text{L}_2(\text{SO}_4)]$ may be displayed by the following steps:

$$\frac{-d[\text{Ni}^{\text{III}}\text{L}_2(\text{SO}_4)]}{2dt} = k_1 K_1 [\text{Ni}^{\text{III}}\text{L}_2(\text{SO}_4)] [\text{H}_2\text{O}_2] [\text{Cu}^{\text{II}}] + k_2 K_2 K_a [\text{Ni}^{\text{III}}\text{L}_2(\text{SO}_4)] [\text{H}_2\text{O}_2] [\text{Cu}^{\text{II}}] / [\text{H}^+] \quad (7)$$

$$= k_1 K_1 K_f [\text{Ni}^{\text{III}}\text{L}_2] [\text{SO}_4] [\text{H}_2\text{O}_2] [\text{Cu}^{\text{II}}] + k_2 K_2 K_a K_f [\text{Ni}^{\text{III}}\text{L}_2] [\text{SO}_4] [\text{H}_2\text{O}_2] [\text{Cu}^{\text{II}}] / [\text{H}^+] \quad (8)$$

$$k = k_1 K_1 K_f [\text{SO}_4] [\text{Cu}^{\text{II}}] + k_2 K_2 K_a K_f [\text{SO}_4] [\text{Cu}^{\text{II}}] / [\text{H}^+] \quad (9)$$

$$k = k_a + K_a k_b / [\text{H}^+] \quad (10)$$

The rate constants displayed an inverse acid dependence as shown in figure 1 and table 1. In the rate law equation (10), $k_a (= k_1 K_1 K_f [\text{Cu}^{\text{II}}] [\text{SO}_4])$ and $k_b K_a (= k_2 K_2 K_f [\text{Cu}^{\text{II}}] [\text{SO}_4])$ were obtained from the intercept and slope, respectively, of the plot of k against $[\text{H}^+]^{-1}$. In spite of the fact, that the reduction potential of $[\text{NiL}_1(\text{SO}_4)]^+$ (0.77V) is less than that of $[\text{NiL}_2(\text{SO}_4)]^+$ (0.81V),³⁷ the oxidation of hydrogen peroxide by $[\text{Ni}^{\text{III}}\text{L}_2]$ was found to be faster than that by $[\text{Ni}^{\text{III}}\text{L}_1]$ in presence of sulphate ion in the pH range $1 < \text{pH} < 2.5$ studied.

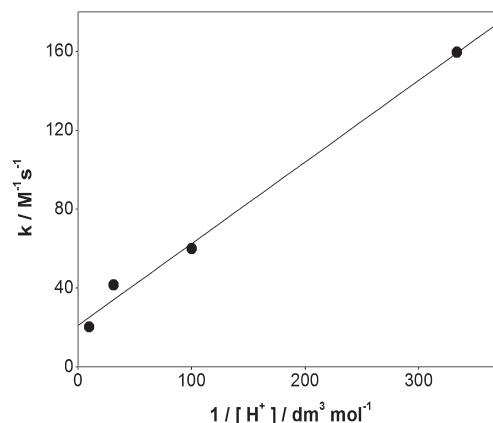


Figure 1. Plot of k against $1/[\text{H}^+]$: $[\text{Ni}(\text{III})] = 5 \times 10^{-5} \text{ mol dm}^{-3}$; $[\text{H}_2\text{O}_2] = 2.5 \times 10^{-4} \text{ mol dm}^{-3}$; $[\text{Na}_2\text{SO}_4] = 0.005 \text{ mol dm}^{-3}$; $I = 0.50 \text{ mol dm}^{-3}$ (NaClO_4); $[\text{Cu}(\text{II})] = 1 \times 10^{-4} \text{ mol dm}^{-3}$; $T = 25^\circ\text{C}$.

Table 1. Dependence of rate on pH. $[\text{Complex}] = 5 \times 10^{-5} \text{ mol dm}^{-3}$; $[\text{H}_2\text{O}_2] = 2.5 \times 10^{-5} \text{ mol dm}^{-3}$; $T = 25^\circ\text{C}$; $[\text{Cu}(\text{II})] = 1 \times 10^{-4} \text{ mol dm}^{-3}$; $[\text{Na}_2\text{SO}_4] = 0.005 \text{ mol dm}^{-3}$; $I = 0.50 \text{ mol dm}^{-3}$ (NaClO_4).

pH	$k / \text{dm}^3 \text{ mol}^{-1} \text{ s}^{-1}$	$k_b K_a / [\text{H}^+]$
1.0	20.3 ± 0.02 (25.3)	4.15
1.5	41.5 ± 0.01 (34.2)	13.0
2.0	60.0 ± 0.01 (62.7)	41.5
2.5	160 ± 0.03 (159)	138

Numbers in parentheses are values calculated with use of (10)

3.1 Interpretation of Reaction Mechanism

The spectral scans for the oxidation of $[\text{NiL}_2](\text{ClO}_4)_2$ with hydrogen peroxide shows a peak at 270 nm with a shoulder near 325 nm and the latter tends to decrease continuously and reaches a limit at 270 nm (figure 2a). The same behaviour is observed after the complete conversion of Ni(III) to Ni(II) in the presence of excess hydrogen peroxide in the reaction medium. With $[\text{Ni}^{\text{III}}\text{L}_1]$, a pink species with an intense peak at 520 nm was observed.³⁴

Oxidation of $[\text{Ni}^{\text{II}}\text{L}_2]$ in aqueous medium in the presence of sulphate concentration of 0.1 mol dm^{-3} was carried under pseudo-first order conditions using an excess of *t*-Butyl hydroperoxide (100-300 fold) at pH = 1 with a constant ionic strength of 0.5 mol dm^{-3} using sodium perchlorate (figure 2b). An intense band (LMCT) appeared at 290 nm, suggesting the formation of Ni(III). The 290 nm band continued to increase in intensity with time with increasing absorbance of LMCT. During the reaction, the intensity of the charge transfer band at 210 nm (CTTS) decreased with time, showing an isobestic point at 240 nm. The pseudo-first order rate constants, k_{obs} , were calculated from the slopes of the linear regression plots $[2 + \log(A_{\alpha} - A_t)]$ versus time of LMCT band. The value of k_{obs} increased with increase of $[t\text{-BuOOH}]$ (table 2, figure 3). The above reaction was very slow in perchlorate and the peak corresponding to Ni(III) was centred at 300 nm. In the presence of sulphate, the LMCT band was more intense than in the presence of perchlorate, which could be expected as the coordination of later may be prevented in the presence of water. The spectral observations were similar in the absence of sulphate. However, the reaction of hydrogen peroxide with this complex shows a peak at 278 nm which is due to the attack of

Table 2. Reaction of $[\text{NiL}_2]^{2+}$ with *t*-BuOOH at pH = 1. $[\text{Ni}^{\text{II}}\text{L}_2] = 5 \times 10^{-5} \text{ mol dm}^{-3}$; $T = 25^\circ\text{C}$; $[\text{Na}_2\text{SO}_4] = 0.1 \text{ mol dm}^{-3}$; $I = 0.50 \text{ mol dm}^{-3}$ (NaClO_4).

$[t\text{-BuOOH}] / \text{mol dm}^{-3}$	$k_{\text{obs}}/10^{-4}, \text{s}^{-1}$
5.00×10^{-3}	2.18 ± 0.02
7.50×10^{-3}	2.67 ± 0.04
1.00×10^{-2}	3.11 ± 0.03
1.25×10^{-2}	3.67 ± 0.02
1.50×10^{-2}	4.40 ± 0.01

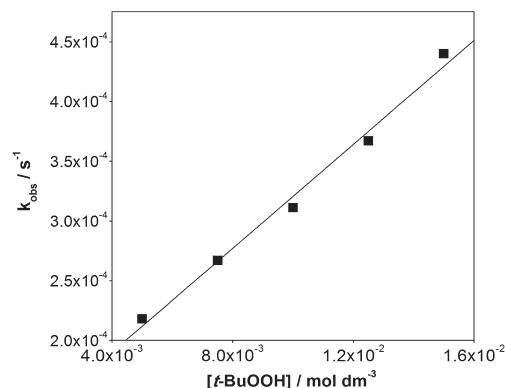


Figure 3. Plot of k_{obs} vs $[t\text{-BuOOH}]$ for the oxidation of $[\text{Ni}^{\text{II}}\text{L}_2]$ by *t*-Butyl hydroperoxide at 25°C : $[\text{Complex}] = 5 \times 10^{-5} \text{ mol dm}^{-3}$; $[\text{Na}_2\text{SO}_4] = 0.1 \text{ mol dm}^{-3}$; pH = 1 (HClO_4); $I = 0.50 \text{ mol dm}^{-3}$ (NaClO_4).

the $\cdot\text{OH}$ radical on the macrocyclic ligand leading to the formation of the unsaturated ligand.

The study shows that the presence of uncoordinated bridge head nitrogen with hydroxyethyl substituent, leads to oxidation of the hexa-aza macrocyclic ring to form a diene instead of a tetraene as in the case of the cyclam ligand.³⁴ In the presence of Cu(II) ions, there is

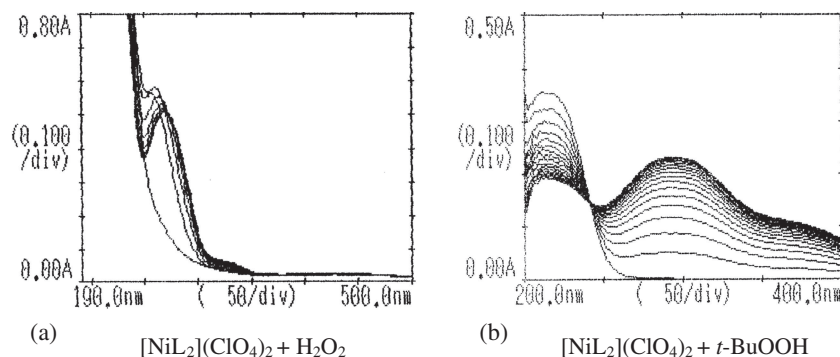


Figure 2. Spectral scans observed for the oxidation of $[\text{NiL}_2](\text{ClO}_4)_2$ with hydrogen peroxide and *t*-butyl hydroperoxide: Reaction condition; pH = 1 (HClO_4); $I = 0.50 \text{ mol dm}^{-3}$ (NaClO_4); (a) complex = $5 \times 10^{-4} \text{ mol dm}^{-3}$; $[\text{H}_2\text{O}_2] = 4 \times 10^{-3} \text{ mol dm}^{-3}$; $[\text{Na}_2\text{SO}_4] = 0.001 \text{ mol dm}^{-3}$ (b) complex = $5 \times 10^{-5} \text{ mol dm}^{-3}$; $[t\text{-BuOOH}] = 5 \times 10^{-3} \text{ mol dm}^{-3}$; $[\text{Na}_2\text{SO}_4] = 0.1 \text{ mol dm}^{-3}$. Scans (a) and (b) measured at 900 second intervals.

no possibility of formation of stable Ni^{3+} species.³⁴ In the presence of Cu(II) , metal centred reduction is predominant rather than the oxidation of macrocyclic ligands. This was also proved by carrying out the oxidation of respective nickel(II)-macrocyclic complex with hydrogen peroxide. Instead of Ni(III) species exhibiting peak at 300 nm, a peak at 270 nm is observed due to a transient species formed. The evidence for the above is given in figure 2a. The transient species formed by the abstraction of H from secondary amino nitrogen of hexa-aza macrocyclic ligand leads to the formation of the diene in aqueous medium.

3.2 Quantum Chemical Studies

3.2a Optimized Geometries of the Ni(II) and Ni(III) Complexes: The present structural optimization study shows that the *trans* III configuration is the most stable

structure in all the six complexes **1-6**, in agreement with the earlier observation in Ni cyclam complexes.^{5,8,29,63} In the *trans* III arrangement, the two six-membered chelating rings in the equatorial part of the complex exhibit chair form and there is centre of symmetry. The optimized *trans*-III conformer possesses C_{2h} point group in the Ni(II) complexes **1** and **4** [$\text{Ni}^{\text{II}}\text{L}$] ($\text{L} = \text{L}_1, \text{L}_2$) while in the Ni(III) complexes the symmetry is lost on account of Jahn-Teller distortion due to the presence of an unpaired electron. Figures 4 and 5 show the optimized geometries of the *trans* III conformation of the complexes **1-6**, as predicted by the BP86/def2-TZVP calculations in aqueous medium. Selected bond lengths, bond angles and dihedral angles for the complexes are given in table 3. As the experimental studies reported in this paper were carried out in aqueous environment, we present here the DFT results obtained in the aqueous medium using the COSMO method. The

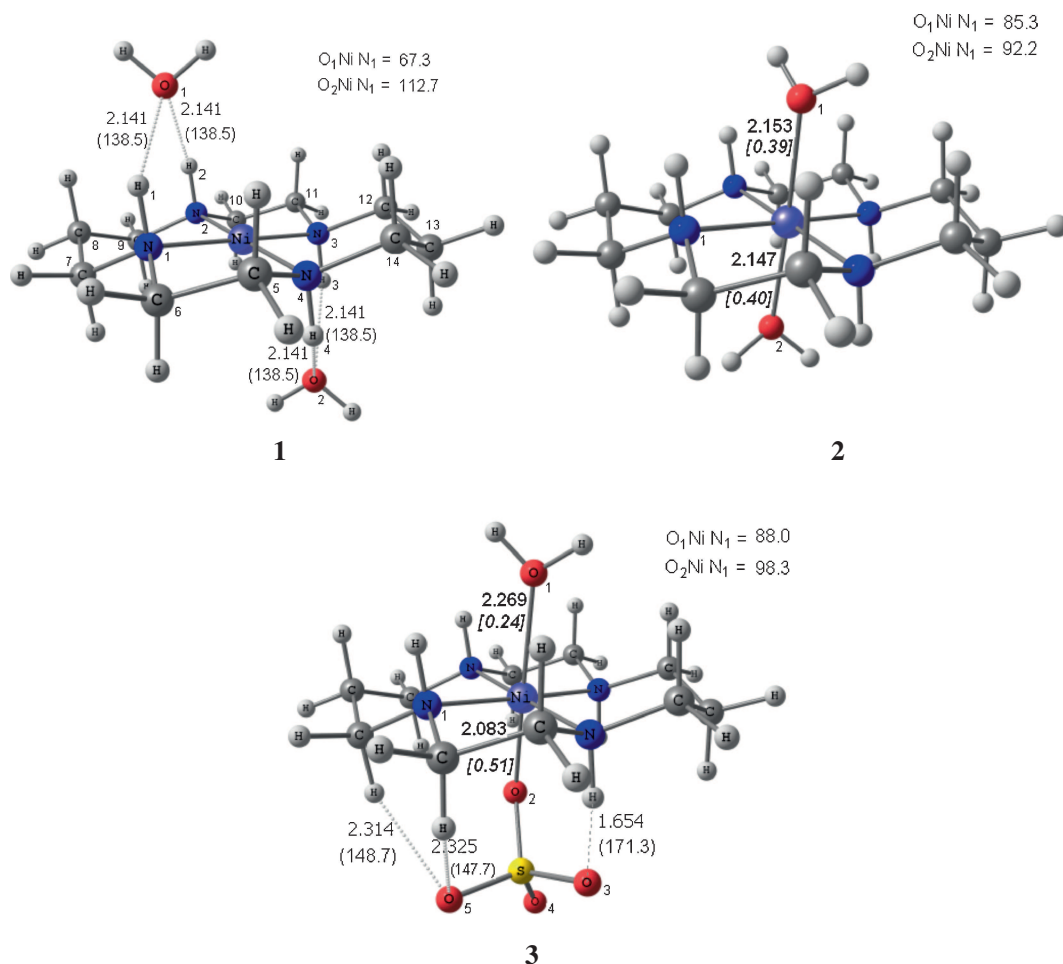


Figure 4. Geometries of Ni(II) and Ni(III)-tetraazamacrocyclic complexes in aqueous medium, optimized at BP86/def2-TZVP level using COSMO method. Labelling of atoms is shown in system **1**. Hydrogen bonds are shown in dotted lines. Hydrogen bond lengths in Å and hydrogen bond angles in degrees (inside parenthesis) are given. The coordinate bond length between the axial water/sulphato ligand with Ni ion is shown in bold and the corresponding covalent bond order is given in italics.

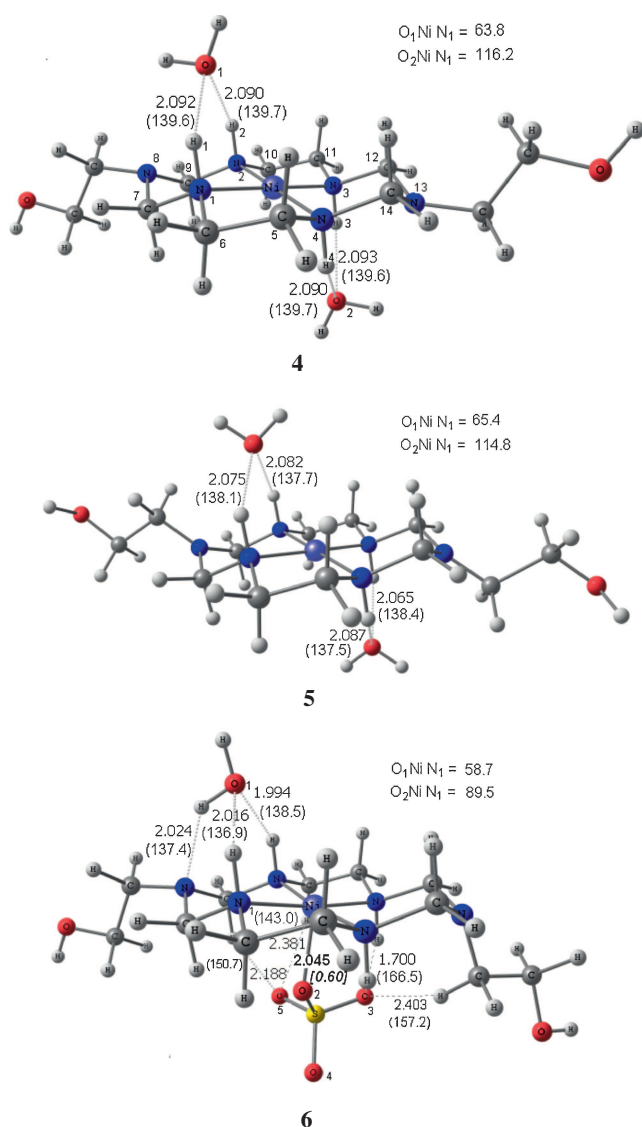


Figure 5. Geometries of Ni(II) and Ni(III)-hexaazamacrocyclic complexes in aqueous medium, optimized at BP86/def2-TZVP level using COSMO method. Labelling of atoms is shown in system **4**. Hydrogen bonds are shown in dotted lines. Hydrogen bond lengths in Å and hydrogen bond angles in degrees (inside parenthesis) are given. The coordinate bond length between the axial sulphato ligand with Ni ion is shown in bold and the corresponding covalent bond order is given in italics.

results obtained in the gas-phase calculations are shown in Supplementary Information.

3.2b Bonding between the Ni(II) and Ni(III) ions and the macrocyclic ligands: In the dicationic complexes **1** and **4**, Ni(II) lies in the centre of the macrocyclic ring and the coordinating nitrogen atoms N_1 , N_2 , N_3 and N_4 are equidistant from the Ni(II) centre. The BP86 study in the aqueous medium predicts that the Ni(II)-N distances in these complexes are 1.951 and 1.938

Å respectively (table 3). The above equatorial Ni(II)-N lengths are significantly shorter than the value of 2.06 Å, observed in the octahedral structure of the high spin $[\text{Ni}(\text{H}_2\text{O})_2(\text{cyclam})]^{2+}$ complex.⁵ The predicted equatorial Ni(II)-N lengths in the present study are characteristic of Ni(II) low-spin complexes. In both the complexes **1** and **4**, Ni(II) is coplanar with the four coordinating N atoms N_1 , N_2 , N_3 and N_4 of the macrocyclic ligand, as revealed by the dihedral angle of 0° for N_1 - N_2 - N_3 - N_4 as well as Ni- N_1 - N_2 - N_3 , etc. All the N-N-N bond angles are 90° in **1** and **4**. The bite angles N-Ni-N involving the six and five membered rings are respectively 93.4 and 86.6° in **1** and 93.2 and 86.8° in **4** which are in agreement with the observed values in Ni-cyclam complexes.^{5,29,37,63,64} The Ni(III) complexes **2**, **3**, **5** and **6** possess C_1 point group. The coordinate Ni(III)-N bond lengths are elongated by about 0.03–0.05 Å in **2** and **3** as compared to the Ni(II)-N lengths in **1**. The predicted Ni(III)-N lengths of ~ 1.977 – 1.997 Å in **2** and **3** agree closely with the mean equatorial Ni-N distance of 1.973 ± 0.006 Å observed in $[\text{NiL}_1(\text{NO}_3)_2]^+$.³⁵

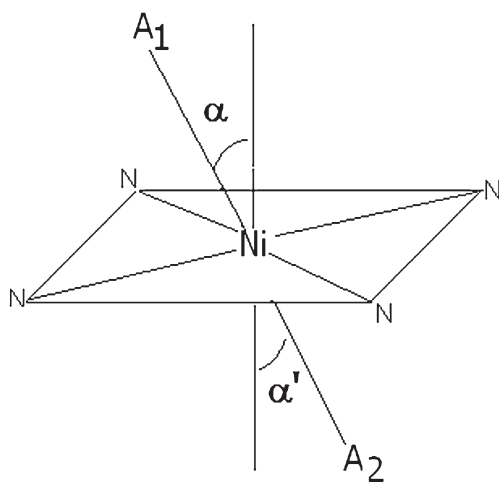
The optimized geometries show that the Ni(III)-N bond lengths are shorter (1.942 Å) in **5** and its structure is very similar to the corresponding symmetric dicationic complex **4**. In the sulphato complex **6**, Ni(III)-N bond lengths are increased by about 0.02–0.03 Å. The DFT study shows that the equatorial Ni-N coordinate bonds possess covalent bond orders in the range 0.63–0.70 (table 3). Thus the Ni-N coordinate bond strength between the nickel ions Ni(II)/Ni(III) and the cyclam/hexaaza macrocyclic ligand is similar in the complexes under study.

The N-N distances in the five-membered chelating rings, N_2 - N_3 and N_1 - N_4 are 2.66–2.73 Å. The predicted distances N_1 - N_2 and N_3 - N_4 in the six-membered rings are longer in the range 2.82–2.92 Å in the complexes **1–6** (table 3). The Ni ion and the ligating nitrogen atoms do not deviate significantly from planarity in these complexes, as the dihedral angles N_1 - N_2 - N_3 - N_4 and Ni- N_1 - N_2 - N_3 are within 1° , with an exception in **6** wherein the Ni(III) is nonplanar by about 4° from the plane of the nitrogen atoms. Further, it is found that the N-N-N angles in the above complexes are around 90° . Thus it is seen that the Ni(II) as well as Ni(III) have a near square planar environment with the four coordinating nitrogen atoms of the macrocyclic ligand.

3.2c Bonding between the Ni(II) and Ni(III) ions and the aqua ligands: The BP86 structural optimization study reveals that the two water molecules in the dicationic Ni(II) complexes **1** and **4**, are tilted from the vertical axis, as seen in figures 4 and 5 and illustrated

Table 3. Selected structural parameters in the complexes **1-6** in aqueous medium by COSMO calculations optimized at BP86/def2-TZVP level. The values inside parentheses correspond to covalent bond orders.

parameter	1	2	3	4	5	6
bond lengths in Å (<i>bond orders</i>)						
Ni-N1	1.951 (0.68)	1.997 (0.65)	1.983 (0.67)	1.938 (0.68)	1.942 (0.70)	1.967 (0.69)
Ni-N2	1.951 (0.68)	1.998 (0.66)	1.996 (0.65)	1.938 (0.68)	1.942 (0.70)	1.957 (0.70)
Ni-N3	1.951 (0.68)	1.996 (0.66)	1.989 (0.63)	1.938 (0.68)	1.942 (0.70)	1.962 (0.69)
Ni-N4	1.951 (0.68)	1.997 (0.65)	1.977 (0.67)	1.938 (0.68)	1.942 (0.70)	1.970 (0.67)
Ni-O1	3.151	2.153 (0.39)	2.269 (0.24)	3.250	3.144	3.336
Ni-O2	3.151	2.147 (0.40)	2.083 (0.51)	3.250	3.146	2.045 (0.60)
N1-N2	2.839	2.912	2.899	2.816	2.831	2.834
N3-N4	2.839	2.921	2.902	2.816	2.830	2.890
N2-N3	2.677	2.730	2.723	2.664	2.658	2.677
N1-N4	2.677	2.727	2.705	2.664	2.660	2.684
Bond angles and dihedral angles (°)						
N1-Ni-N2	93.4	93.6	93.5	93.2	93.6	92.5
N3-Ni-N4	93.4	94.1	94.1	93.2	93.6	94.6
N2-Ni-N3	86.6	86.2	86.2	86.8	86.4	86.2
N4-Ni-N1	86.6	86.1	86.2	86.8	86.4	85.9
N1-N2-N3	90.0	90.1	89.8	90.0	90.0	90.7
N1-N2-N3-N4	0.0	0.8	-0.1	0.0	0.1	-1.0
Ni-N1-N2-N3	0.0	-0.6	-0.9	0.0	0.0	-4.4

**Figure 6.** Definition of the tilt angles α and α' illustrating the orientations of the axial ligands A_1 (H_2O) and A_2 (H_2O/SO_4^{2-}) in the Ni complexes.

in figure 6. In these dicationic complexes the bond angles O_1NiN_1 and O_2NiN_1 deviate significantly from 90° expected in a regular octahedral arrangement. These angles are, respectively, 67.3 and 112.7° in **1** and reveal that the water molecules are tilted by $\alpha = \alpha' = 22.7^\circ$ from the vertical axis (table 4). In **4**, the water molecules are tilted more (tilt angle $\alpha = \alpha' = 26.2^\circ$). Due to the above tilting, the oxygen atoms of the water molecules are closer to the secondary NH hydrogen atoms of the macrocyclic ligand. Analysis of the optimized geometries show that in **1** and **4**, the

acceptor oxygen of the water ligand is positioned vertically above (or below) the mid-point between the pair of NH hydrogen atoms in the macrocyclic ligand. Thus the aqua oxygen O_1 forms two hydrogen bonds with H_1 and H_2 of the macrocyclic ligand (figures 4 and 5). Similarly, oxygen O_2 forms H-bonds with H_3 and H_4 . The resulting four H-bonds have same lengths and angles in view of the C_{2h} symmetry in **1** and **4**. The H-bond lengths are 2.14 \AA and the H-bond angles are 138.5° in **1** (figure 4). The hydroxy ethyl substituted bridge head nitrogens in **4** lead to shortening of the H-bond lengths by $\sim 0.05 \text{ \AA}$ and widening of the H-bond angle by $\sim 1^\circ$ (figure 5) as compared to that in **1**. The H-bond lengths and angles predicted in **1** and **4** are characteristic of weak H-bonds.⁶⁵⁻⁶⁷ The distance between the Ni(II) ion and the oxygen atom of the water molecule is $>3.1 \text{ \AA}$ (table 3) and it is evident that there is no coordinate bond formation between the Ni ion and the water ligands in **1** and **4**. The present COSMO calculations in aqueous medium at the BP86/def2-TVZP level show that the two water ligands are bound to $[Ni^{II}L]$, $L = L_1$ and L_2 , through hydrogen bonding interactions with the equatorial macrocyclic ligand, L. The gas-phase calculations at the BP86/def2-TVZP as well as B3LYP/6-31+G* levels also lead to the same conclusion on the above Ni(II) complexes as reflected by the tilt angles shown in table 4 figures S1 and S3 and tables S2 and S3 (Supporting Information). It is evident that Ni(II) complexes **1** and **4** are dihydrates represented as $[Ni^{II}L_1].2H_2O$ and $[Ni^{II}L_2].2H_2O$ respectively. The two

hydrated water molecules are located in the vicinity of the macrocyclic ligand as suggested by Ito *et al.*¹⁷

In contrast, in the Ni(III) cyclam complex $[\text{Ni}^{\text{III}}\text{L}_1]$ (**2**), there is a small tilting of aqua ligands from the vertical axis. The water molecule A_1 (figure 6) is tilted by $\alpha = 4.7^\circ$ while the second water molecule A_2 is tilted by $\alpha' = 2.2^\circ$ from the vertical axis (table 4). The BP86 COSMO calculations on the nickel(III) complex **2** reveal that there is coordinate covalent bond between Ni and the axial water ligands A_1 and A_2 (figure 4) as reflected by the Ni-O₁ and Ni-O₂ distances of 2.153 Å and 2.147 Å, respectively, having covalent bond orders of 0.39 and 0.40. Thus the tricationic cyclam complex **2** possesses the octahedral structure $[\text{Ni}^{\text{III}}\text{L}_1(\text{H}_2\text{O})_2]$. The axial Ni(III)-O bond lengths are ~ 0.02 Å shorter than the corresponding value of 2.176 Å in the crystal structure of the high spin Ni(II) complex $[\text{NiL}_1(\text{H}_2\text{O})_2]\text{Cl}_2 \cdot 4\text{H}_2\text{O}$.⁵ The axial Ni(III)-O bonds (bond order ~ 0.40) in $[\text{NiL}_1(\text{H}_2\text{O})_2]^{3+}$ (**2**) are weaker than the equatorial Ni(III)-N bonds (bond order ~ 0.65). This prediction is in agreement with the observation of elongated geometry in Ni(III) species with axial coordination of the solvent or counter-ions as confirmed by hyperfine interactions.^{3,25}

However, the structure of the analogous hexaaza-macrocyclic Ni(III) complex **5** is quite similar to that of the corresponding dicationic complex **4** $[\text{Ni}^{\text{II}}\text{L}_2] \cdot 2\text{H}_2\text{O}$. The water ligands in **5** are tilted considerably ($\alpha = 24.6^\circ$; $\alpha' = 24.8^\circ$) and they participate in H-bond formation with the macrocyclic ligand L_2 , similar to that in **4**. The BP86 study predicts that there is no coordinate bond formation between the water ligands and Ni(III) in complex **5** unlike in the analogous complex **2** $[\text{Ni}^{\text{III}}\text{L}_1(\text{H}_2\text{O})_2]$, though the electronic environment of Ni(III) is similar in these two complexes. The difference in the modes of bonding of the axial water molecules with Ni(III) may be attributed to the effect of macrocyclic equatorial ligands. Spectroscopic studies of Kobiro *et al.* on Ni(II) alkyl-substituted cyclam complexes⁶⁸ reveal that in the sterically congested cyclam complexes, cyclam ring would prevent

axial water molecules from interacting with the deeply embedded Ni^{2+} ion. It was found that tetramethylethane subunits in cyclam ligand would hinder axial ligands such as nitrate anions or water molecules from accessing the central Ni(II) ion. Absence of coordinate bond formation between the water molecule and Ni(III) in **5** may be due to the presence of hydroxyethyl substituents in the bridgehead nitrogen atoms of the hexaazamacrocyclic ligand L_2 . The present analysis reveals that **5** exists as a dihydrate $[\text{Ni}^{\text{III}}\text{L}_2] \cdot 2\text{H}_2\text{O}$ similar to the dicationic complex **4** $[\text{Ni}^{\text{II}}\text{L}_2] \cdot 2\text{H}_2\text{O}$.

Our analysis leads to the inference that $[\text{Ni}^{\text{III}}\text{L}_1(\text{H}_2\text{O})_2]$ is more stable complex than $[\text{Ni}^{\text{III}}\text{L}_2] \cdot 2\text{H}_2\text{O}$ in view of the presence of the coordinately bound water molecules in the former whereas there is no coordinate bonding between the water ligands and Ni(III) in the latter.

3.2d Nature of bonding between Ni(III) and the axial ligands in the sulphato complexes: The DFT study shows that in the sulphato complexes, **3** and **6**, the sulphato anion is bound to the Ni(III) cation in the axial position by coordinate bond formation through the sulphato oxygen atom O₂ (figures 4 and 5). The Ni(III)-O₂ bond lengths are 2.083 and 2.045 Å, respectively, when the equatorial ligands are L_1 and L_2 . These bond lengths are significantly shorter than the Ni-O bond lengths^{24,25} of ~ 2.11 Å in the $[\text{Ni}(\text{cyclam})(\text{NO}_3)_2]^+$ and the DFT predicted values in $[\text{Ni}^{\text{III}}\text{L}_1(\text{H}_2\text{O})_2]$ (2.153 and 2.147 Å). The Ni(III)-O bond lengths in the sulphato complexes **3** and **6** agree with the crystallographic values of 2.048 and 2.074 Å, observed for the axial bonds in phosphate complexes.²⁹ Our analysis leads to the inference that the coordinate bond between Ni(III) and the sulphate ligand in **3** and **6** is stronger than those of the axial coordinate bonds with water in **2**. This is substantiated by the higher bond orders of 0.51 and 0.60 in **3** and **6**, respectively, for the Ni(III)-sulphato bonds as compared to the values of 0.39 and 0.40 for the Ni(III)-aqua bonds in **2**. It is striking to note that the strength of the coordinate bond between the Ni^{3+} and sulphate anion in **6** $[\text{Ni}^{\text{III}}\text{L}_2(\text{SO}_4)]$ having covalent bond order of 0.60 is quite similar to the equatorial Ni-N coordinate bonds (bond orders $\sim 0.63 - 0.70$). It is of interest to note that the coordinating oxygen atom of the sulphato ligand is positioned vertically below the Ni(III) ion in **6** (with a very small tilt angle $\alpha' = 0.5^\circ$), whereas in **3** it is tilted by 8.3° . It is interesting to note that $[\text{Ni}(\text{II})\text{L}_1]$ also forms axial coordination with sulphate through bridging oxygen.⁶⁹ In addition to the formation of axial coordinate bond, the sulphato oxygen atoms O₃ and O₅ in **3** and **6** participate in H-bonding interactions with C-H / N-H hydrogens of the macrocyclic ligand (figures 4 and

Table 4. Tilt angles (in degrees) for the axial ligands in the complexes **1–6** predicted by BP86/def2-TZVP calculations in aqueous medium and gas-phase.

Tilt angle	1	2	3	4	5	6
Aqueous phase (COSMO method)						
α	22.7	4.7	2.0	26.2	24.6	31.3
α'	22.7	2.2	8.3	26.2	24.8	0.5
Gas- phase						
α	24.3	26.8	27.0	26.5	25.6	34.1
α'	24.3	7.2	13.9	26.5	25.7	8.4

5). Besides, in **6** the hydroxyethyl chain bonded to the tertiary nitrogen N₁₃ bends towards the sulphato group such that there is H-bond between O₃ and one of the methylenic hydrogens (figure 5) having H-bond length and angle of 2.403 Å and 157.2°, respectively.

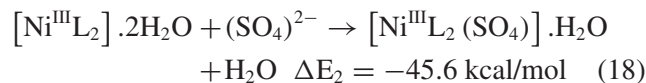
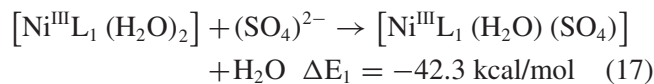
Analysis of bonding involving the axial water molecule reveals a striking difference in the mode of bonding in **3** and **6**. The water molecule is coordinately bound in the axial position in **3** with Ni(III)-O₁ bond length 2.269 Å and the corresponding bond order is 0.24. The above axial bond is elongated by ~0.1 Å as compared to that in **2** and is in agreement with the shorter bond order of 0.24. It may be noted that the covalent bond orders of about 0.2-0.5 were predicted between the ligating atom and the metal centre in different coordination compounds by earlier quantum chemical studies.⁷⁰⁻⁷³

It is observed that the water molecule in **6** is bound in the complex through three hydrogen bonding interactions, two of which are between the aqua oxygen O₁ and the NH hydrogens H₁ and H₂ as observed in **1**, **4** and **5**. The additional H-bond between the water ligand and the hexaaza macrocyclic ring arises due to larger tilting ($\alpha = 31.4^\circ$) of the water from the vertical axis. The resulting orientation of the water in **6** leads to a new H-bond between one of the hydrogen atoms of water and the tertiary bridge-head nitrogen N₈ as seen in figure 5. Lack of coordinate bond formation between water molecule and Ni(III) in **6** may be attributed to the macrocyclic ligand effect as observed in the case of **5**. Based on these results, the structure of **3** and **6** may be assigned as [Ni^{III}L₁(SO₄)(H₂O)] and [Ni^{III}L₂(SO₄)].H₂O respectively.

The BP86/def2-TZVP structural optimisation using the COSMO model to account for the solvent effect indeed predicts the structure and mode of bonding in the Ni(II)/Ni(III) complexes that agree with the experimental observations. The BP86/def2-TZVP gas-phase results given in the Supplementary Information (figures S1 and S2, table S2) also predict the same trends in the bonding modes in Ni(II) complexes **1** and **4** and Ni(III) complexes **5** and **6**. However the gas-phase study does not lead to coordinate bond formation of the axial water A1 in the complexes **2** and **3** as seen from the large tilt angle α (table 4) which results in hydrogen bonding interactions with L₁. The B3LYP/6-31+G* gas-phase calculations could not account for the coordinate bond formation between Ni(III) and the sulphate anion in **6** (figure S4 and table S3).

3.2e Stability of the Sulphato complexes: We have examined the stability of the sulphate complexes **3** and

6 by examining the energetic of the reactions given below:



From the total energies of the reactants and products (table S1), it is seen that the reactions 17 and 18 are exothermic by 42.3 and 45.6 kcal/mol respectively. Energy considerations reveal that the formation of the sulphato complexes **3** and **6** from the tricationic aquo complexes **2** and **5** are favored thermodynamically.

4. Conclusions

In summary, kinetics of oxidation of H₂O₂ by [Ni^{III}L₂(SO₄)].H₂O catalysed by Cu(II) ions led to the metal centred reduction and was found to be faster than that by [Ni^{III}L₁(H₂O)(SO₄)]. Quantum chemical calculations reveal that in aqueous medium coordinate bond formation between Ni and the axial water ligands in [Ni^{III}L₁(H₂O)₂] and [Ni^{III}L₁(H₂O)(SO₄)] contributes to stability of the complexes. However, in the corresponding complexes of the hexaaza macrocyclic ligand L₂, [Ni^{III}L₂].2H₂O and [Ni^{III}L₂(SO₄)].(H₂O), the water molecules are hydrated and are stabilized through weak hydrogen bonding with L₂. This explains the shorter life time of complex [Ni^{III}L₂].2H₂O as compared to [Ni^{III}L₁(H₂O)₂]. The presence of the weak H-bonding interactions due to hydrated water in [Ni^{III}L₂(SO₄)].(H₂O) accounts for its faster kinetics of oxidation of H₂O₂ as compared to [Ni^{III}L₁(H₂O)(SO₄)]. Structure and bonding analyses of the sulphate complexes reveal that the larger tilting of axial water in [Ni^{III}L₂(SO₄)].H₂O leads to a hydrogen bond formation between one of the tertiary nitrogen atoms of L₂ and a hydrogen atom of water ligand.

Supplementary Information

Additional results from quantum chemical studies including total energies of optimized geometries (table S1), structures in the gas-phase (figures S1-S4), selected structural parameters (tables S2 and S3) and Cartesian coordinates of the optimized geometries in the aqueous and gas-phase are available at www.ias.ac.in/chemsci.

Acknowledgements

EJPM thanks High Power Computing Facility, Centre for Molecular Simulation and Design, University of Hyderabad for providing partial support of the computational work. The optimized geometries of the complexes (figures 4 and 5 and S1–S4) were generated using the software CHEMCRAFT (<http://www.chemcraftprog.com>) which is duly acknowledged.

References

1. Telser J, Horng Y C, Becker D F, Hoffman B M and Ragsdale S W 2000 *J. Am. Chem. Soc.* **122** 182
2. Zeigerson E, Ginzburg G, Kirschenbaum L J and Meyerstein D 1981 *J. Electroanal. Chem.* **127** 113
3. Haines R I and McAuley A 1980 *Inorg. Chem.* **19** 719
4. Fairbank M G, McAuley A, Norman P R and Olubuyide O 1985 *Can. J. Chem.* **63** 2983
5. Mochizuki K and Kondo T 1995 *Inorg. Chem.* **34** 6241
6. Hancock R D and McDougall G J 1980 *J. Am. Chem. Soc.* **102** 6551
7. Thom V J, Fox C C, Boeyens J C A and Hancock R D 1984 *J. Am. Chem. Soc.* **106** 5947
8. Choi K Y, Kim Y J, Ryu H and Suh I H 1999 *Inorg. Chem. Commun.* **2** 176
9. Choi K Y, Choi S N and Suh I H 1998 *Polyhydron* **17** 1415
10. Kang S G, Ryu K, Jung S K and Kim J 1999 *Inorg. Chim. Acta* **292** 140
11. Choi H J, Lee T S and Suh M P 1999 *Angew. Chem. Int. Ed.* **38** 1405
12. Choi K Y, Ryu H, Lee K C, Lee H H, Hong C P, Kim J H and Sung N D 2003 *Bull. Korean. Chem. Soc.* **24** 1150
13. Fabbrizzi L, Perotti A, Profumo A and Soldi T 1986 *Inorg. Chem.* **25** 4256
14. Anichini A, Fabbrizzi L, Paoletti P and Clay R M 1977 *Inorg. Chim. Acta* **24** L21
15. Ciampolini M, Fabbrizzi L, Licchelli M, Perotti A, Pezzini F and Poggi A 1986 *Inorg. Chem.* **25** 4131
16. Barefield E K, Bianchi A, Billo E J, Conndly P J, Paoletti P, Summers J S and Van Derveer D G 1986 *Inorg. Chem.* **25** 4197
17. Ito T, Toriumi K and Ito H 1981 *Bull. Chem. Soc. Jpn.* **54** 1096
18. Gore E S and Busch D H 1973 *Inorg. Chem.* **12** 1
19. Koola J D and Kochi J K 1987 *Inorg. Chem.* **26** 908
20. Kineary J F, Roy T M, Albert J S, Yoon H, Wagler T R, Shen L and Burrows C J 1989 *J. Inclus. Phenom.* **7** 155
21. Yoon H, Wagler T R, O'Connor K J and Burrows C J 1990 *J. Am. Chem. Soc.* **112** 4568
22. Roslonek G and Taraszewska J 1992 *J. Electroanal. Chem.* **325** 285
23. Muller J G, Chen X, Diaz A C, Rokita S E and Burrows C J 1993 *Pure Appl. Chem.* **65** 545
24. Halcrow M A. and Christou G 1994 *Chem. Rev.* **94** 2421
25. Zeigerson E, Ginzburg G, Schwartz N, Luz Z and Meyerstein D 1979 *J. Chem. Soc. Chem. Commun.* 241
26. Zeigerson E, Ginzburg G, Meyerstein D and Kirschenbaum L J 1980 *J. Chem. Soc. Dalton Trans.* 1243
27. Zeigerson E, Ginzburg G, Becker J Y, Kirschenbaum L J, Cohen H and Meyerstein D 1981 *Inorg. Chem.* **20** 3988
28. Zeigerson E, Ginzburg G, Kirschenbaum L J and Meyerstein D 1981 *J. Electroanal. Chem.* **127** 113
29. Zeigerson E, Bar I, Bernstein J, Kirschenbaum L J and Meyerstein D 1982 *Inorg. Chem.* **21** 73
30. Kim J C, Lough A J and Kim H 2002 *Inorg. Chem. Commun.* **5** 771
31. Choi K Y, Suh I H and Hong C P 1999 *Inorg. Chem. Commun.* **2** 604
32. Lindoy L F, Mahina M S, Skelton B W and White A H 2003 *J. Coord. Chem.* **56** 1203
33. Zilbermann I, Meshulam A, Cohen H and Meyerstein D 1993 *Inorg. Chim. Acta* **206** 127
34. Anuradha S and Vijayaraghavan V R 2013 *J. Chem. Sci.* **125** 1123
35. McAuley A, Palmer T and Whitcombe T W 1993 *Can. J. Chem.* **71** 1792
36. Fabbrizzi L 1979 *J. Chem. Soc., Dalton Trans.* 1857
37. Suh M P, Shim B Y and Yoon T 1994 *Inorg. Chem.* **33** 5509
38. Anuradha S and Vijayaraghavan V R 2010 *React. Kinet. Mech. Cat.* **101** 279
39. Suh M P, Lee E Y and Shim B Y 1998 *Inorg. Chim. Acta* **269** 337
40. (a) Becke A D 1988 *Phys. Rev. A* **38** 3098; (b) Perdew J P 1986 *Phys. Rev. B* **33** 8822
41. Weigend F and Ahlrichs R 2005 *Phys. Chem. Chem. Phys.* **7** 3297
42. Schweinfurth D, Krzystek J, Schapiro I, Demeshko S, Klein J, Telser J, Ozarowski A, Su C Y, Meyer F, Atanasov M, Neese F and Sarkar B 2013 *Inorg. Chem.* **52** 6880
43. Petrenko T, Ray K, Wieghardt K E and Neese F 2006 *J. Am. Chem. Soc.* **128** 4422
44. Izsak R and Neese F 2011 *J. Chem. Phys.* **135** 144105
45. Kossmann S and Neese F 2010 *J. Chem. Theory Comput.* **6** 2325
46. Kossmann S and Neese F 2009 *Chem. Phys. Lett.* **481** 240
47. Neese F, Wennmohs F, Hansen A and Becker U 2009 *Chem. Phys.* **356** 98
48. Neese F 2003 *J. Comp. Chem.* **24** 1740
49. Neese F 2012 *WIREs Comput. Mol. Sci.* **2** 73
50. Klamt A and Schütürmann G 1993 *J. Chem. Soc., Perkin Trans.* **2** 799
51. Grimme S, Antony J, Ehrlich S and Krieg H 2010 *J. Chem. Phys.* **132** 154104
52. Grimme S 2011 *WIREs Comput. Mol. Sci.* **1** 211
53. (a) Mayer I 1983 *Chem. Phys. Lett.* **97** 270; (b) Mayer I 1984 *Int. J. Quant. Chem.* **26** 151; (c) Mayer I 1985 *Theor. Chim. Acta* **67** 315
54. (a) Becke A D 1993 *J. Chem. Phys.* **98** 5648; (b) Lee C, Yang W and Parr R G 1988 *Phys. Rev. B* **37** 785

55. M J Frisch, *et al.*, 2004 *GAUSSIAN 03*, Revision E.01, Gaussian, Inc., Wallingford CT
56. Espenson J H 1995 In *Chemical Kinetics and Reaction Mechanisms* 2nd ed (New York: McGraw-Hill)
57. Brodovitch J C, McAuley A and Oswald T 1982 *Inorg. Chem.* **21** 3442
58. Macartney D H 1986 *Can. J. Chem.* **64** 1936
59. Koshino N, Funahashi S and Takagi H D 1997 *J. Chem. Soc. Dalton Trans.* 4175
60. Burg A, Maimon E, Cohen H and Meyerstein D 2007 *Eur. J. Inorg. Chem.* 530
61. Haber F and Weiss J 1934 *J. Proc. Roy. Soc. (London)* **A147** 332
62. Barb W G, Baxendale J H, George P and Hargrave K R 1951 *Trans. Faraday Soc.* **47** 591
63. Bosnich B, Poon C K and Tobe M L 1965 *Inorg. Chem.* **4** 1102
64. Prasad L and Nyburg S C 1987 *Acta Cryst. C* **43** 1038
65. Desiraju G R and Steiner T 2001 In *The weak hydrogen bond: In structural chemistry and biology* (Oxford: Oxford University Press)
66. Jeffrey G A 1997 In *An Introduction to Hydrogen Bonding* (Topics in Physical Chemistry) (Oxford: Oxford University Press)
67. Parthasarathi R, Subramanian V and Sathayamurthy N 2006 *J. Phys. Chem. A* **110** 3349
68. Kobiro K, Nakayama A, Hiro T, Suwa M and Tobe Y 1992 *Inorg. Chem.* **31** 676
69. Churchard A J, Cyranski M K and Grochala W 2010 *Acta Cryst. C* **66** m263
70. Malar E J P 2004 *Eur. J. Inorg. Chem.* 2723
71. Malar E J P 2005 *Theoret. Chem. Acc.* **114** 213
72. Malar E J P 2003 *Inorg. Chem.* **42** 3873
73. Calvi A O, Aullon G, Alvarez S, Montero L A and Stohrer W D 2006 *J. Mol. Structure: Theochem.* **767** 37